Chemical Science

Accepted Manuscript

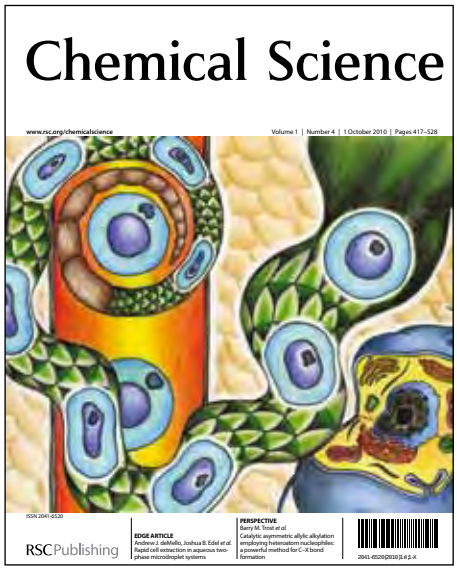

This is an *Accepted Manuscript*, which has been through the RSC Publishing peer review process and has been accepted for publication.

Accepted Manuscripts are published online shortly after acceptance, which is prior to technical editing, formatting and proof reading. This free service from RSC Publishing allows authors to make their results available to the community, in citable form, before publication of the edited article. This *Accepted Manuscript* will be replaced by the edited and formatted *Advance Article* as soon as this is available.

To cite this manuscript please use its permanent Digital Object Identifier (DOI®), which is identical for all formats of publication.

More information about *Accepted Manuscripts* can be found in the **Information for Authors**.

Please note that technical editing may introduce minor changes to the text and/or graphics contained in the manuscript submitted by the author(s) which may alter content, and that the standard **Terms & Conditions** and the **ethical guidelines** that apply to the journal are still applicable. In no event shall the RSC be held responsible for any errors or omissions in these *Accepted Manuscript* manuscripts or any consequences arising from the use of any information contained in them.

Cite this: DOI: 10.1039/c0xx00000x

www.rsc.org/chemicalscience

EDGE ARTICLE

Benzene-Fused BODIPY and Fully-Fused BODIPY Dimer: Impacts of the Ring-Fusing at the *b* Bond in the BODIPY Skeleton

Atsushi Wakamiya,*[a] Takanori Murakami[b] and Shigehiro Yamaguchi*[b]

Received (in XXX, XXX) Xth XXXXXXXXX 20XX, Accepted Xth XXXXXXXXX 20XX

DOI: 10.1039/b000000x

4,4-Difluoro-4-bora-3a,4a-diaza-*s*-indacenes (BODIPYs) are fascinating dyes with great potentials for various applications. To establish the design principle for the modification of the BODIPY skeleton, we now investigate the electronic impacts of the introduction of ring-fused structures. The DFT calculations revealed that while the benzene-fusing at the *a* bond in the BODIPY skeleton increases the HOMO level, the benzene-fusing at the *b* bond leads to a decreased LUMO level. Based on these results, a benzo[*b*]-fused BODIPY **1** and a fully-fused BODIPY dimer **2** were synthesized. X-ray crystal structure analysis demonstrated that the benzo[*b*]-fused structure significantly perturbs the π-conjugation with enhancement of an electron-accepting azafluvene character. In the ring-fused BODIPY dimer **2**, the central benzene ring is largely deviated from the aromatic benzene geometry. As a consequence, **2** has a significantly low-lying LUMO delocalized along the periphery. In cyclic voltammograms, the benzene-fused BODIPY **1** and fully-fused dimer **2** indeed showed reversible reduction waves at much less negative potentials ($E_{1/2}$ = –1.05 V vs Fc/Fc^+ for **1**, –0.85 V for **2**), relative to a non-fused BODDIPY **3** ($E_{1/2}$ = –1.40 V). In addition, the benzene-fused BODIPYs showed broad and intense absorption bands in the Vis-NIR region. In particular, the BODIPY dimer **2** showed an intense absorption at 629 nm with a broad shoulder band reaching 900 nm. Corresponding to the red-shifted absorption, compounds **1** and **2** showed week fluorescence in deep red region (λ_{em} = 690 nm, Φ_F <0.01) and in near-infrared region (940 nm, Φ_F <0.01), respectively.

Introduction

BODIPYs, 4,4-difluoro-4-bora-3a,4a-diaza-*s*-indacenes, are fascinating dyes with some notable features, such as an excellent stability, intense absorption profiles, and insensitivity to the polarity of the environment.[1] Various structural modifications of the BODIPY skeleton at the periphery[2] or at the boron atom[3] have been extensively studied in order to alter their photophysical properties, and, thereby, their significant utilities in a variety of applications, including fluorescent probes for biomolecules,[4] photodynamic therapy,[5] laser dyes,[6] emissive materials in OLEDs,[7] and organic photovoltaics,[8] have been demonstrated. Among them, a particularly urgent challenge is the application to organic photovoltaics as the dyes absorbing light in the near infrared (NIR) region.[9] For the molecular design of narrow HOMO-LUMO gap dyes, decreasing the LUMO level while

[a] *Institute for Chemical Research, Kyoto University and PRESTO, JST, Gokasho, Uji, Kyoto, 611-0011, Japan. Fax: 81 774 38 3178; Tel: 81 38 3173; E-mail:wakamiya@scl.kyoto-u.ac.jp*

[b] *Department of Chemistry, Graduate School of Science, and Research Center for Materials Science, Nagoya University and CREST, JST, Chikusa, Nagoya, 464-8602, Japan. E-mail: yamaguchi@chem.nagoya-u.ac.jp*

†Electronic Supplementary Information (ESI) available: Experimental procedures, analytical data for compounds prepared in this work. CCDC reference numbers 899844–899846. For ESI and crystallographic data in CIF or other electronic format see DOI: 10.1039/b000000x/

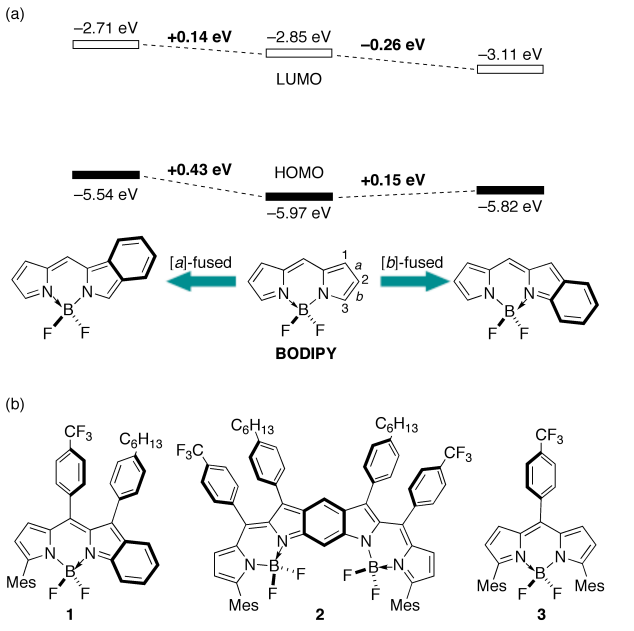

Fig. 1 Benzene-fused BODIPYs: (a) Effect of the benzene-fused structures on the electronic structures (B3LYP/6-31G(d)) and (b) structures of the BODIPY derivatives synthesized in this study.

maintaining a moderate increment of the HOMO level is important for the stability toward air oxidation. To this end, how to efficiently expand the π conjugation is a key issue. Whereas the direct dimerization or oligomerization at the 2- or 3-position of the BODIPY skeleton might be a straightforward way, this often suffers from steric congestion caused by neighboring substituents, resulting in a twisted non-coplanar conformation.[10] As part of our chemistry of the fully ring-fused planar π-conjugated materials,[11] we are now interested in introducing the fused structure to the BODIPY skeleton.[12–14] While several derivatives having the fused structures at the *a* bond have been reported,[12] the *b* bond-fused derivatives are still limited to only a few examples,[13] such as the difurano[*b*,*g*]-fused derivatives. We now disclose the synthesis of benzo[*b*]-fused BODIPY **1** and its dimer **2** consisting of 7 fully-fused rings (Fig. 1). Based on the study of their structure properties relationships, we will discuss the impacts of the *b* bond-fused structure.

We first elucidated how the benzene-fused structure alters the electronic structure of the BODIPY skeleton. The DFT calculations at the B3LYP/6-31G(d) level of theory revealed that the electronic structure is highly dependent on the position where the benzene ring is fused. While the benzene-fusing at the *a* bond in the BODIPY skeleton increases the HOMO energy level, the benzene-fusing at the *b* bond leads to a decreased LUMO level along with a slight increase in the HOMO level, as shown in Fig. 1. Consequently, the benzo[*b*]-fused derivative has a narrower HOMO–LUMO gap. The BODIPY skeleton can be regarded as a combination of the electron-donating pyrrole and electron-accepting azafulvene moieties. The aforementioned effects may be interpreted such that, while the benzo[*a*]-fused structure enhances the character of the benzo[*c*]pyrrole substructure, thereby resulting in the destabilization of the HOMO energy level, the benzo[*b*]-fused structure enhances the azafulvene character to decrease the LUMO level and make the HOMO–LUMO gap narrower while maintaining a moderate increment of the HOMO level. These electronic effects of the benzo[*b*]-fused structure would be beneficial to the molecular design of air-stable NIR dyes. To demonstrate the validity of the design, we experimentally investigated the benzo[*b*]-fused derivatives **1** and **2**, in which the *p*-CF_3- and *p*-hexyl-substituted phenyl groups were introduced on the peripheral positions in order to increase the electron-accepting ability and solubility, respectively. As a reference compound, we also examined a non-benzene-fused BODIPY **3** (Fig. 1).

Results and discussion

Synthesis of a series of benzo[*b*]-fused BODIPY derivatives

The synthesis of unsymmetrically substituted BODIPYs is generally achieved based on the condensation of a ketopyrrole with another pyrrole in the presence of acid.[1] According to this methodology, we first attempted the synthesis of the benzene-fused BODIPY **1**. However, the reaction of the indole **4** with ketopyrrole **6** in the presence of trifluoroacetic acid only produced **1** in poor yield (~3%), probably due to the lower electrophilicity of the indole at the 2-position compared to that of the pyrrole (ESI). Therefore, we examined alternative routes and finally obtained **1** by the direct nucleophilic reaction of a 2-lithioindole derivative with the ketopyrrole, as shown in Scheme 1. Thus, starting from the *N*-Boc-indole derivative **4**, the ortho-metalation using EtZn(μ-Et)(μ-TMP)Li as a base[15] followed by treatment with I_2 produced a 2-iodoindole derivative **5**. Lithiation of **5** with *t*-BuLi generated a 2-lithioindole derivative, which was reacted with the ketopyrrole **6** to give a hydroxy derivative **7**. Without isolation, this compound was successively treated with CF_3COOH in CH_2Cl_2 and $BF_3{\cdot}OEt_2$ in the presence of Et_3N. Purification by silica gel column chromatography gave us the benzene-fused BODIPY **1** in 34% yield (overall for the 3 steps) as a dark purple solid. On the basis of this methodology, using benzodipyrrole **8** as the starting material, the benzene-fused BODIPY dimer **2** was also successfully synthesized in 20% yield (overall for the 3 steps) as a dark green solid. Both compounds **1** and **2** are stable toward air and water and soluble in the common organic solvents, such as $CHCl_3$ and THF. Compound **3** was also

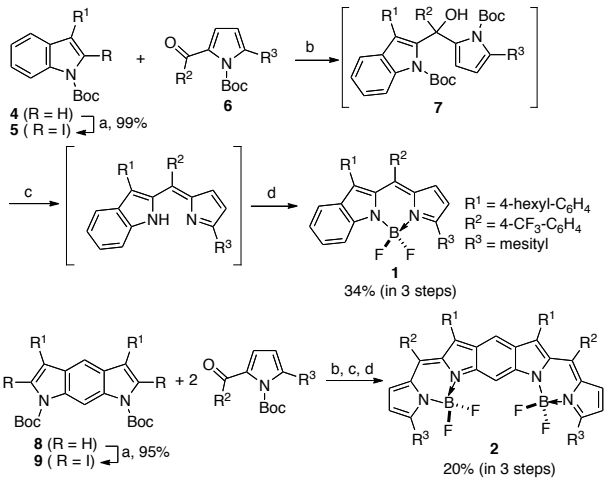

Scheme 1 *Reagents and conditions*: (a) EtZn(μ-Et)(μ-TMP)Li, THF, –78 °C, then I_2; (b) *t*-BuLi, THF, –78 °C; (c) CF_3COOH, CH_2Cl_2, rt.; (d) $BF_3{\cdot}OEt_2$, Et_3N, toluene, reflux.

prepared according to the conventional method (see ESI).

Structural features of benzo[*b*]-fused BODIPY derivatives

The effect of the benzene-fused structure in compound **1** was first studied based on the X-ray structure analysis. As shown in Fig. 2a, the BODIPY skeleton has a planar structure with the torsion angles among the fused four ring skeletons of less than 6.1°. The terminal mesityl group is arranged nearly perpendicular to the BODIPY plane, while the other aryl groups at the C5 and C7 positions are arranged with the tilt angles of 57.2° and 54.7°, respectively. Notably, the bond distances (Å) of C1–N1 (1.349(3)), C2–C3 (1.360(4)), and C4–C5 (1.388(4)) are substantially shorter than those of C9–N2 (1.374(3)), C7–C8 (1.425(4)), and C5–C6 (1.423(4)), respectively. These differences indicate the more significant contribution of form **A** between two possible resonance structures, as shown in Fig. 2b. The form **A** is a canonical structure that consists of the aromatic benzene and azafluvene substructures.

This consideration is supported by the quantum chemical calculations. Thus, the structural optimization for a model compound **1′** (R^1 = tolyl) calculated at the B3LYP/6-31G(d) level of theory well reproduced the crystal structure (ESI). The NICS(0) values for the optimized structure calculated at the HF/6-31+G(d,p) level are summarized in Fig. 2c. The NICS(0) value for the terminal pyrrole ring is –6.6, which is less negative than that (–9.6) of the pyrrole ring in the indole substructure and, moreover, even compared to that of the pyrrole ring (–8.0) in the non-benzene-fused derivative **3**. This result implies that the nonaromatic azafulvene character is enhanced by introducing the benzo[*b*]-fused structure in **1**. However, the NICS(0) values for the benzene (–7.8) and pyrrole (–9.6) rings of the indole substructure in **1′** are also less negative compared to those of the benzene (–11.3) and pyrrole (–13.2) rings in the parent indole. This fact suggests that the form **B**, which has a quinoid structure for the indole moiety, should also contribute to some extent to the resonance equilibrium.

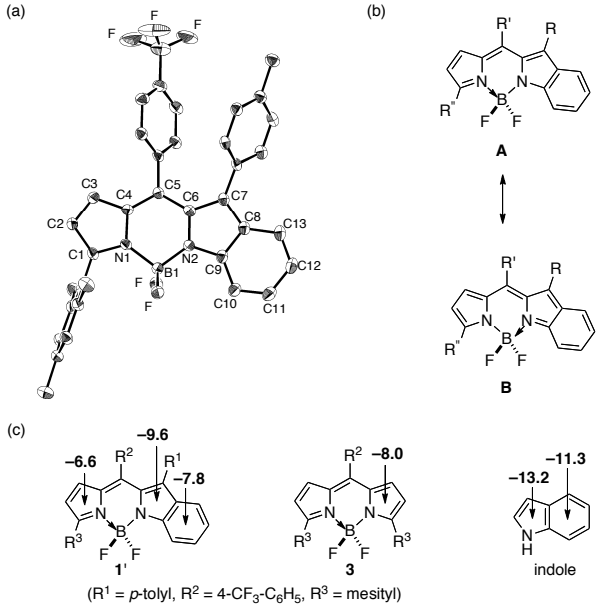

Fig. 2 Structural features and aromaticity in **1**: (a) *ORTEP* drawing (50% probability for thermal ellipsoids), where the pentyl group is omitted for clarity; (b) resonance structures; (c) NICS(0) values (ppm) for **1′**, **3**, and indole, calculated at the HF/6-31+G(d,p)//B3LYP/6-31G(d) level.

A similar structural feature was also observed in the crystal structure of the 7-ring fused dimer **2** (Fig. 3a). This compound has a symmetrical plane at the center of the molecule. The bond distances (Å) of C1–N1 (1.340(4)), C2–C3 (1.367(5)), C4–C5 (1.383(5)) are shorter than those of C9–N2 (1.368(4)), C7–C8 (1.434(4)), and C5–C6 (1.417(5)), respectively (Fig. 3). These results again demonstrate that the azafulvene character is enhanced in both of the terminal pyrrole rings by the introduction of the benzene-fused structure. In addition, it is worth noting that the bond distance of C8–C9 (1.443(4)) is substantially longer than those of C8–C11 (1.395(4)) and C9–C10 (1.387(4)). This implies that the central benzene ring in the BODIPY dimer significantly deviates from the aromatic benzene geometry and,

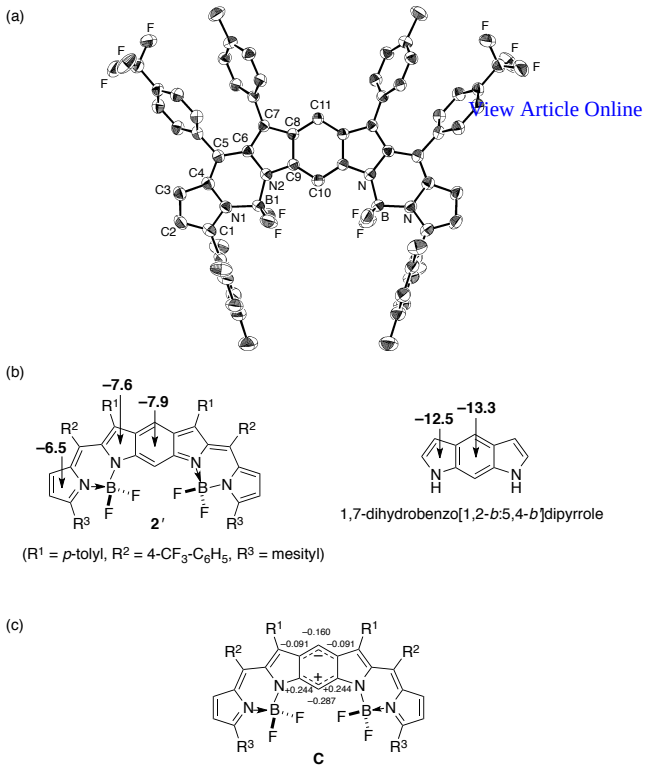

Fig. 3 Structural features and aromaticity in **2**: (a) *ORTEP* drawing (50% probability for thermal ellipsoids), where the pentyl group is omitted for clarity; (b) NICS(0) values (ppm) for **2′** and 1,7-dihydrobenzo[1,2-*b*:5,4-*b′*]dipyrrole calculated at the HF/6-31+G(d,p)//B3LYP/6-31G(d) level; (c) a representation of the resonance structure with a quinoid character. The atomic charges on the benzene rings for **2′** obtained by NPA (B3LYP/6-31G(d) are included.

instead, the quinoid character is enhanced in the benzodipyrrole moiety.

Electronic Structures of benzo[*b*]-fused BODIPY derivatives

These structural features of **2** were reproduced in the optimized structure (B3LYP/6-31G(d)) for a model compound **2′** (R^1 = tolyl), which also showed a substantial bond alternation in the central benzene ring (ESI). The NICS(0) values calculated for the terminal pyrrole ring and the central benzene ring (HF/6-31+G(d,p)) are –6.5 and –7.9, respectively. These values are much less negative compared to those for the pyrrole ring (–8.0) in the parent BODIPY **3** and the benzene ring (–13.3) in the parent benzodipyrroles, implying the lower aromaticity in these ring skeletons. The natural population analysis (NPA) (B3LYP/6-31G(d)) showed a deflection in the atomic charges on the benzene ring in **2′** as shown in Fig. 3c. Taking these results into account, the structure of **2** might be best depicted as form **C** in Fig. 3c, which has the characteristics of the terminal azafulvene substructures and the zwitterionic character of the central benzodipyrrole substructure. In conjunction with this consideration, the calculations also indicated the interesting electronic structure of compound **2′** as shown in Fig. 4. The LUMO of **2′** is delocalized along the periphery and consequently lies in a substantially lower energy level compared to that of **1′**.

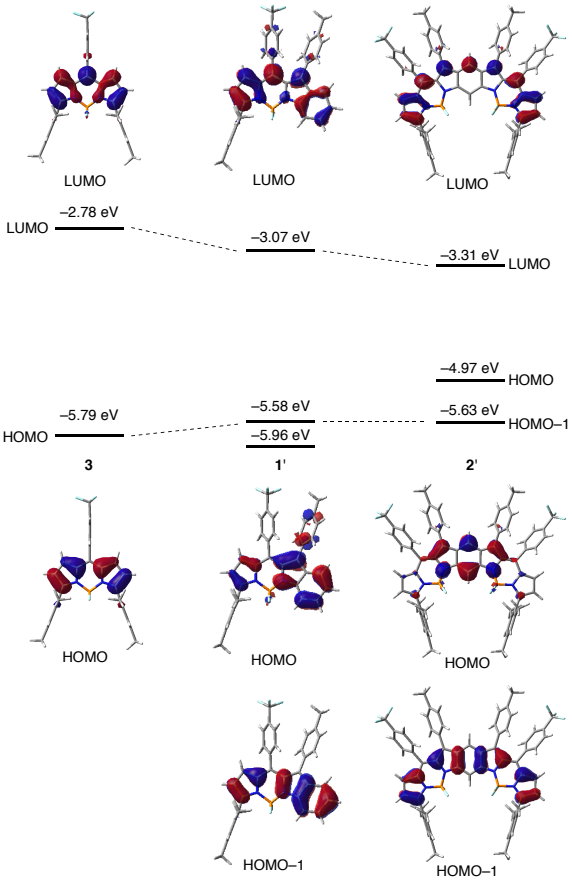

Fig. 4 Pictorial presentation of the frontier orbitals and a plot of the Kohn-Sham HOMOs and LUMO energy levels for **1′**–**3** (B3LYP/6-31G(d)).

In the occupied molecular orbitals, beside the inherent π-orbital of the BODIPY skeleton that appeared as the HOMO–1, **2′** has a higher-lying HOMO that originated from the benzodipyrrole skeleton.

Based on the structural features, the benzene-fusing at the *b* bond in the BODIPY skeleton significantly alters the electronic structure. In particular, the dimerization of the BODIPY skeletons through the benzene-fused structure is effective to attain the narrow HOMO–LUMO gap. These electronic effects indeed result in several characteristic electrochemical and photophysical properties.

Impacts of the Benzo[b]-fusing on Electrochemical Properties

Fig. 5 shows the cyclic voltammograms of **1** and **2**, together with that of **3** for comparison, which were measured in CH_2Cl_2 with $(n\text{-Bu})_4NPF_6$ as the supporting electrolyte. In comparison with the non-fused BODIPY **3**, while the benzo[*b*]-fused **1** showed an irreversible oxidation wave at only a slightly less positive potential, it exhibited a reversible reduction process at a much less negative potential by 0.35 V. This comparison demonstrates that the benzene-fused structure at the *b* bond is indeed effective to decrease the LUMO level. In the oxidation process for **1**, the new weak oxidation peaks at around 0.80 V and +0.20 V appeared after the oxidation process at +1.05 V (ESI). This result implies that **1** might undergo electropolymerization

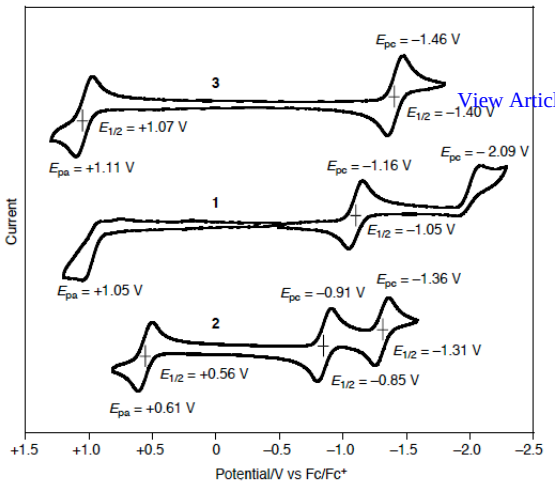

Fig. 5 Cyclic voltammograms of **1**–**3** in CH_2Cl_2 (1 mM), measured with $(n\text{-Bu})_4N^+PF_6^-$ (0.1 M) as a supporting electrolyte at a scan rate of 100 mVs^{-1}.

upon oxidation at the unprotected terminal benzene ring. On the other hand, the benzene-fused dimer **2** showed both reversible oxidation and reduction processes at the significantly less positive and less negative potentials of $E_{1/2}$ = +0.56 V and –0.85 V, respectively. The differences between these values and those for **3** amount to –0.51 and +0.55 V, respectively, demonstrating the significant impacts of the dimerization through the benzene-fused structure. Notably, the first reduction potential of the dimer **2** is less negative even compared to that of C_{60} ($E_{1/2}$ = –0.98 V vs Fc/Fc^+),[16] indicative of its potential use as an electron-accepting material. In addition, the dimer **2** also showed a reversible second reduction process at $E_{1/2}$ = –1.31 V, suggesting the formation of stable reduced species to the dianion under the stated measurement conditions.

Impacts of the Benzo[b]-fusing on Photophysical Properties

Fig. 6 shows the Vis-NIR absorption spectra of compounds **1**–**3** in THF. While the non-fused BODIPY **3** showed an intense absorption band with the maximum (λ_{max}) at 519 nm (log ε = 4.80), the benzo[*b*]-fused derivative **1** showed a relatively broad band at λ_{max} = 539 nm (log ε = 4.73), which is red-shifted by 20

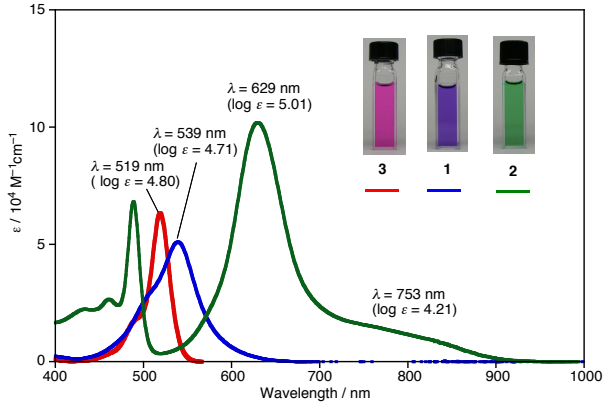

Fig. 6 UV-vis-NIR absorption spectra of **1**–**3** in THF with their absorption data. The pictures of their THF solutions are included.

nm relative to **3**. The band of **1** is broadened to 620 nm, which makes the color of the solution of **1** reddish-purple as shown in Fig 6. A more striking difference was observed for the benzene-fused dimer **2**. Thus, this compound showed a very intense absorption band at the more red-shifted λ_{max} of 629 nm with a significantly high molar extinction coefficient (ε) of 1.0×10^5 $M^{-1}cm^{-1}$, and, in addition, a broad shoulder band with a tail up to 900 nm with the ε of 1.5×10^4 $M^{-1}cm^{-1}$. These features are beneficial to absorbing light in the long wavelength region when used as a dye for photovoltaics. According to the TD-DFT calculations of the model compound **2′** (B3LYP/6-31G(d)), while the intense absorption at λ_{max} = 629 nm is assignable to the transition from the HOMO–1 to the LUMO, the broad absorption band in the near IR region is attributed to the transition from the HOMO to the LUMO (Fig. 4, ESI). The absorption spectra of **1** and **2** were insensitive to the solvents (**1**: 543 nm in cyclohexane, 538 nm in DMF, **2**: 637 and 789 nm in cyclohexane, 622 and 771 nm in DMF, ESI), indicative of small difference in their dipole moments between the ground state and the excited state. In the fluorescence spectra in THF, compounds **1** and **2** showed week emissions in deep red region (λ_{em} = 690 nm, Φ_F <0.01) and in near-infrared region (940 nm, Φ_F <0.01), respectively (ESI). The reference compound **3** also showed a week emission at λ_{em} = 550 nm (Φ_F = 0.02). One reason for the low fluorescence quantum yields in these compounds is probably due to the rotation of aryl group on the peripheral positions in the BODIPY skeleton.[2b]

Conclusions

In summary, the impacts of the ring-fusing in the BODIPY skeleton is highly dependent on the position at which the ring is introduced. The benzene-fusing at the *b* bond is an effective way to decrease the LUMO level. In particular, the dimerization of the BODIPY skeleton through the benzene-fused structure significantly alters the electronic structure by attaining a low-lying LUMO as well as the narrow HOMO–LUMO gap. The produced compound showed intriguing electrochemical and photophysical properties, such as the NIR absorption. These results would provide an important guideline for further structural modification of the BODIPY frameworks. Further synthetic study of more extended BODIPY oligomers with the benzene-fused structure is now in progress in our laboratory.

Acknowledgements

We thank Prof. M. Minoura at Kitasato University and Prof. T. Sasamori at Kyoto University for valuable suggestions on X-ray crystal structure analysis of compound **3**. This work was supported by Grants-in-Aid (19685004 and 19675001) from the Ministry of Education, Culture, Sports, Science, and Technology, Japan.

References

1 (a) A. Loudet and K. Burgess, *Chem. Rev*. 2007, **107**, 4891; (b) R. Ziessel, G. Ulrich and A. Harriman, *New. J. Chem.* 2007, **31**, 496; (c) G. Ulrich, R. Ziessel and A. Harriman, *Angew. Chem. Int. Ed*. 2008, **47**, 1184.

2 (a) K. Rurack, M. Kollmannsberger and J. Daub, *Angew. Chem. Int. Ed.* 2001, **40**, 385; (b) A. Wakamiya, N. Sugita and S. Yamaguchi, *Chem. Lett*. 2008, **37**, 1094; (c) T. Sakida, S. Yamaguchi and H. Shinokubo, *Angew. Chem. Int. Ed.* 2011, **50**, 2280; (d) J.-s. Lu, H. Fu, Y. Zhang, Z. J. Jakubek, Y. Tao and S. Wang, *Angew. Chem. Int. Ed.* 2011, **50**, 11658.

3 (a) G. Ulrich, C. Goze, M. Guardigli, A. Roda and R. Ziessel, *Angew. Chem., Int. Ed*. 2005, **44**, 3694; (b) C. Goze, G. Ulrich, L. J. Mallon, B. D. Allen, A. Harriman and R. Ziessel, *J. Am. Chem. Soc*. 2006, **128**, 10231; (c) T. Bura, P. Retailleau and R. Ziessel, *Angew. Chem. Int. Ed*. 2010, **49**, 6659.

4 Y. Urano, D. Asanuma, Y. Hama, Y. Koyama, T. Barrett, M. Kamiya, T. Nagano, T. Watanabe, A. Hasegawa, P. L. Choyke and H. Kobayashi, *Nature Med*. 2009, **15,** 104.

5 T. Yogo, Y. Urano, Y. Ishitsuka, F. Maniwa, T. Nagano, *J. Am. Chem. Soc*. 2005, **127**, 12162.

6 M. Shah, K. Thangraj, M.-L. Soong, L. T. Wolford, J. H. Boyer, I. R. Politzer and T. G. Pavlopoulos, *Heteroat. Chem*. 1990, **1**, 389.

7 L. Bonardi, H. Kanaan, F. Camerel, P. Jolinat, P. Retailleau and R. Ziessel, *Adv. Funct. Mater*. 2008, **18**, 401.

8 (a) S. Hattori, K. Ohkubo, Y. Urano, H. Sunahara, T. Nagano, Y. Wada, N. V. Tkachenko, H. Lemmetyinen and S. Fukuzumi, *J. Phys. Chem. B* 2005, **109**, 15368; (b) S. Erten-Ela, M. D. Yilmaz, B. Icli, Y. Dede, S. Icli and E. U. Akkaya, *Org. Lett*. 2008, **10**, 3299; (c) T. Rousseau, A. Cravino, T. Bura, G. Ulrich, R. Ziessel and J. Roncali, *Chem. Commun.* 2009, 1673; (d) D. Kumaresan, R. P. Thummel, T. Bura, G. Ulrich and R. Ziessel, *Chem. Eur. J.* 2009, **15**, 6335; (e) Y. Hayashi, N. Obata, M. Tamaru, S. Yamaguchi, Y. Matsuo, A. Saeki, S. Seki, Y. Kureishi, S. Saito, S. Yamaguchi and H. Shinokubo, *Org. Lett*. 2012, **14**, 866.

9 (a) A. Mishra, M. K. R. Fischer and P. Bäuerle, *Angew. Chem. Int. Ed*. 2009, **48**, 2474; (b) P. M. Beaujuge and J. M. J. Fréchet, *J. Am. Chem. Soc.* 2011, **133**, 20009.

10 (a) M. Bröring, R. Krüger, S. Link, C. Kleeberg, S. Köhler, X. Xie, B. Ventura and L. Flamigni, *Chem. Eur. J*. 2008, **14**, 2976; (b) B. Ventura, G. Marconi, M. Bröring, R. Krüger and L. Flamigni; *New. J. Chem*. 2009, **33**, 428.

11 (a) Z. Zhou, A. Wakamiya, T. Kushida and S. Yamaguchi, *J. Am. Chem. Soc*. 2012, **134**, 4529; (b) S. Saito, K. Matsuo and S. Yamaguchi, *J. Am. Chem. Soc*. 2012, **134**, 9130; (c) S. Yamaguchi, C. Xu and T. Okamoto, *Pure Appl. Chem*. 2006, **78**, 721; (d) A. Fukazawa and S. Yamaguchi, *Chem. Asian J*. 2009, **4**, 1386.

12 (a) M. Wada, S. Ito, H. Uno, T. Murashima, N. Ono, T. Urano and Y. Urano, *Tetrahedron Lett.* 2001, **42**, 6711; (b) Z. Shen, H. Röhr, K. Rurack, H. Uno, M. Spieles, B. Schulz, G. Reck and N. Ono, *Chem. Eur. J*. 2004, **10**, 4853; (c) S. Goeb and R. Ziessel, *Org. Lett*. 2007, **9**, 737; (d) A. B. Descalzo, H.-J. Xu, Z.-L. Xue, K. Hoffmann, Z. Shen, M. G. Weller, X.-Z. You and K. Rurack, *Org. Lett.* 2008, **10**, 1581; (e) T. Okujima, Y. Tomimori, J. Nakamura, H. Yamada, H. Uno and N. Ono, *Tetrahedron* 2010, **66**, 6895; (f) C. Yu, Y. Xu, L. Jiao, J. Zhou, Z. Wang and E. Hao, *Chem. Eur. J.* 2012, **18**, 6437; (g) M. Nakamura, H. Tahara, K. Takahashi, T. Nagata, H. Uoyama, D. Kuzuhara, S. Mori, T. Okujima, H. Yamada and H. Uno, *Org. Biomol. Chem*. 2012, **10**, 6840.

13 (a) K. Umezawa, Y. Nakamura, H. Makino, D. Citterio and K. Suzuki, *J. Am. Chem. Soc*. 2008, **130**, 1550; (b) K. Umezawa, A. Matsui, Y. Nakamura, D. Citterio and K. Suzuki, *Chem. Eur. J*. 2009, **15**, 1096; (c) V. Leen, W. Qin, W. Yang, J. Cui, C. Xu, X. Tang, W. Liu, K. Robeyns, L. V. Meervelt, D. Beljonne, R. Lazzaroni, C. Tonnelé, N. Boens and W. Dehaen, *Chem. Asian J*. 2010, **5**, 2016; (d) S. G. Awuah, J. Polreis, V. Biradar and Y. You, *Org. Lett*. 2011, **13**, 3884; (e) C. Zhao, P. Feng, J. Cao, Y. Zhang, X. Wang, Y. Yang, Y. Zhang and J. Zhang, *Org. Biomol. Chem*. 2012, **10**, 267.

14 (a) C. Jiao, K.-W. Huang and J. Wu, *Org. Lett.* 2011, **13**, 632; (b) C. Jiao, L. Zhu and J. Wu, *Chem. Eur. J*. 2011, **17**, 6610; (c) L. Zeng, C. Jiao, X. Huang, K.-W. Huang, W.-S. Chin and J. Wu, *Org. Lett.* 2011, **13**, 6026.

15 Y. Kondo, J. V. Morey, J. C. Morgan, H. Naka, D. Nobuto, P. R. Raithby, M. Uchiyama and A. E. H. Wheatley; *J. Am. Chem. Soc*. 2007, **129**, 12734, and references therein.

16 Q. Xie, E. Pérez-Cordero and L. Echegoyen, *J. Am. Chem. Soc.* 1992, **114**, 3978.

Graphical Abstract: